

# Leaf litter thickness, but not plant species, can affect root detection by ground penetrating radar

Toko Tanikawa · Hidetoshi Ikeno ·  
Masako Dannoura · Keitarou Yamase · Kenji Aono ·  
Yasuhiro Hirano

Received: 30 November 2015 / Accepted: 18 May 2016 / Published online: 25 May 2016  
© Springer International Publishing Switzerland 2016

## Abstract

**Aim** Ground penetrating radar (GPR), a nondestructive tool that can detect coarse tree roots, has not yet become a mature technology for use in forests. In this study, we asked two questions concerning this technology: (i) Does the leaf litter layer influence root detection and major indices based on the time interval between zero crossings ( $T$ ) and the amplitude area ( $A$ )? (ii) Can GPR images discriminate roots of different plant species?

**Methods** Roots buried in a sandy bed, which was covered with different thicknesses of leaf litter, were

scanned using a 900 MHz GPR antenna. Roots of four plant species in the bed were also scanned.

**Results** Leaf litter decreased root reflections without distorting the shape of the hyperbolas in the radar profile.  $A$  values decreased with increasing litter thickness, whereas  $T$  was independent of litter thickness. For all species combined, GPR indices were significantly correlated with root diameter.

**Conclusions** Leaf litter dramatically decreased root detection, but the influence of the litter could be ignored when the sum of  $T$  for all reflection waveforms ( $\Sigma T$ ) is

---

Responsible Editor: Peter J. Gregory.

**Electronic supplementary material** The online version of this article (doi:10.1007/s11104-016-2931-0) contains supplementary material, which is available to authorized users.

---

T. Tanikawa (✉)  
Kansai Research Center, Forestry and Forest Products Research  
Institute, 68 Nagai-kyutaro, Momoyama, Fushimi,  
Kyoto 612-0855, Japan  
e-mail: tanikawa@affrc.go.jp

H. Ikeno  
School of Human Science and Environment, University of Hyogo,  
Hyogo 670-0092, Japan

M. Dannoura  
Graduate School of Global Environmental Studies, Graduate  
School of Agriculture, Kyoto University, Kyoto 606-8502, Japan

K. Yamase  
Hyogo Prefectural Technology Center for Agriculture, Forestry  
and Fisheries, Shiso 671-2515, Japan

K. Aono  
The General Environmental Technos Co., Ltd. (KANSO  
Technos), Osaka 541-0052, Japan

Y. Hirano  
Graduate School of Environmental Studies, Nagoya University,  
Nagoya 464-8601, Japan

adopted to estimate root diameter. To use  $A$  values to detect roots, litter should be removed or equalized in thickness. Radar profiles could not reliably differentiate among roots belonging to plants of different species.

**Keywords** Coarse roots · Leaf litter · Nondestructive root detection · *Phyllostachys pubescens* · Root diameter

### Abbreviations

$A$	Amplitude area
$\Sigma A$	Sum of amplitude areas for all reflection waveforms
Single $A_{\max}$	Amplitude area of the maximum reflection waveform
$T$	Time interval between zero crossings
$\Sigma T$	Sum of time intervals for all reflection waveforms
Single $T_{\max}$	Time interval for the maximum reflection waveform
GPR	Ground penetrating radar

### Introduction

Climate change will greatly increase the frequency, severity, and spatial extent of extreme weather events (IPCC 2012). To evaluate the influence of these changes on terrestrial ecosystems, accurate estimates of tree root biomass and carbon sequestration are required, as roots represent one of the key belowground carbon pools (Brunner and Godbold 2007). Furthermore, structural roots play important mechanical roles in increasing a soil's shear resistance and thereby decreasing landslide frequency (Preston and Crozier 1999; Khalilnejad et al. 2012; Giadrossich et al. 2013; Fan and Lai 2014; Ghestem et al. 2014). This will be important for maintaining slope stability against heavy precipitation, which will be a primary manifestation of climate change in some regions (Groisman et al. 1999; Trenberth 1999). In turn, climate change may alter root depths by affecting soil water availability (Schenk and Jackson 2002). Root systems account for 20 to 40 % of total tree biomass carbon (Dixon et al. 1994; Jackson et al. 1996; Brunner and Godbold 2007; Paul et al. 2008). Thus to evaluate root system structure and biomass, nondestructive root quantification methods such as radioactive tracers, electrical resistance/conductance

tomography, and ground penetrating radar (GPR) have been developed (Butnor et al. 2012).

Ground penetrating radar is an electromagnetic reflection technique for exploration, imaging, characterization, and monitoring of belowground structures (al Hagrey 2012). It allows researchers to characterize buried materials by analyzing the reflected waves and evaluating the spatial distribution of these reflections in the radar profiles (Cheng et al. 2014). This technique produces reflections that resemble hyperbolas in the radar profile (Butnor et al. 2012). The approach is particularly attractive because it utilizes off-the-shelf equipment that is highly portable, rapid to operate, and that can be used to scan large areas daily without requiring root excavation or time-consuming site preparation before measurements (Butnor et al. 2012). These properties make GPR highly suitable for surveys of tree roots in forests, so studies of this application have rapidly increased, both to estimate root biomass (e.g., Butnor et al. 2001, 2003; Cox et al. 2005; Stover et al. 2007; Cui et al. 2011, 2013; Hirano et al. 2012) and to produce three-dimensional maps of the distribution of coarse roots (e.g., Cheng et al. 2014; Wu et al. 2014). Furthermore, GPR can be used simultaneously with other techniques to improve our understanding of various phenomena in belowground ecosystems. For instance, water absorption by the whole tree's root system has been studied by combining GPR with light microscopy and sap flow measurements (Cermak et al. 2000).

However, despite the promise of GPR, its successful application appears to be site-specific (Butnor et al. 2001, 2003). That is, the instrument must be calibrated for each site to provide reliable estimates. To identify factors that could be used to improve its suitability for field studies, we examined the effects of two key problems that make it difficult to reliably detect tree roots in forest ecosystems. When GPR operators arrive at a forest study site, the first problem relates to whether they should remove the leaf litter before scanning for roots. Leaf litter may create reflections that obscure root images; therefore, it is necessary to determine whether roots can be detected through the litter layer. Thus far, the influence of litter on radar profiles has only been qualitatively described by Butnor et al. (2005). They showed that scanning through the leaf litter defocused the GPR radar waves and degraded the radar's ability to detect roots. Because leaf litter may decrease the ability to study large areas of a forest using GPR, it is important

to quantify the effects of leaf litter on the GPR images and indices calculated from this data. The second factor that affects GPR signals in forest ecosystems relates to the roots of co-existing tree species at a site. Previous GPR studies have detected the coarse roots of several tree species, including *Cryptomeria japonica*, *Pinus taeda*, *Pinus thunbergii*, *Prunus persica*, and *Ulmus pumila*, but focused on only one tree species at a given site (Butnor et al. 2003; Cox et al. 2005; Dannoura et al. 2008; Cui et al. 2011; Hirano et al. 2009, 2012; Wu et al. 2014). For application in mixed-species forests, researchers need to know whether GPR can differentiate the tree roots of different species. Although the roots of several tree species are commonly found growing in the same soil volume in forest soils, researchers have not reported whether the different tree species can be identified from the radar profile. Radar images can vary with the root water content (Hirano et al. 2009), and root anatomical traits differ among plant species in the root cross-section (Karizumi 2010). For example, hardwoods possess vessel elements, whereas coniferous trees have tracheid, and *Pinus* spp. have resin canals but *Cryptomeria* spp. do not (Karizumi 2010). Some species of *Phyllostachys* bamboo have several specific types of pore in their rhizome cross-section (Karizumi 2010). The different anatomical traits may induce variations in the travel time and other characteristics of the electromagnetic wave as it passes through the root or rhizome and may therefore affect the resulting signal strength, suggesting that it may be possible to distinguish species. Gormally et al. (2011) showed that the shapes and intensities of the radar reflections from polyvinyl chloride pipes depended on the materials inside the pipes, such as water and air. Therefore, we hypothesized that the radar signal of roots would differ among tree species.

Based on the abovementioned limitations of our current knowledge about GPR, the goals of the present study were to answer two questions: (1) Does leaf litter at the ground surface influence root detection by GPR? (2) Do GPR images and indices differ among the roots of different plant species? To answer these questions, we quantified the influence of the two factors (leaf litter and plant species) on GPR images and on various forms of two major GPR indices related to root diameter, namely the time interval between zero crossings ( $T$ , ns) and the amplitude area ( $A$ , dB  $\times$  ns) (Fig. 1; Tanikawa et al. 2013), under controlled conditions.

## Materials and methods

### Experimental design

We used the sand plot established by Hirano et al. (2009) in the experimental forest at the Kansai Research Center, Forestry and Forest Products Research Institute (FFPRI), Kyoto, Japan. The plot size was  $7 \times 2 \times 1.2$  m. To create the plot before each study, all soil in the plot was removed to a depth of 1.2 m, and the plot was refilled with sand from a granite parent material. All root and rhizome (the subterranean stem of *Phyllostachys pubescens* bamboo) samples used in this study were collected from the experimental field at FFPRI. Each sample was cut from living trees (roots) or bamboo (rhizomes), and then the ends of the cut were immediately sealed with silicone to prevent water loss. A steel pipe was used as a control and was scanned using GPR together with the roots and rhizomes.

Experiment 1–1 was designed to clarify the influence of the litter layer on root identification by GPR. Three *Cryptomeria japonica* roots with diameters of 2.8, 3.6, and 6.3 cm were buried at a depth of 30 cm in the sand bed, separated horizontally at 50-cm intervals (Fig. 2a). The surface of the ground was covered by leaf litter of *C. japonica* with one of five thicknesses: 0 (not covered),  $2.2 \pm 0.9$ ,  $5.0 \pm 1.5$ ,  $6.8 \pm 1.8$ , or  $10.5 \pm 3.0$  cm ( $n = 5$ , mean  $\pm$  standard deviation). The GPR device was placed on the surface (i.e., the bare soil or litter layer), then the roots were scanned three times along a single transect, perpendicular to the long axis of the roots, where the most intensive and clear hyperbolas could be observed (Tanikawa et al. 2013).

Experiment 1–2 was designed to compare the attenuation effects of depth on GPR indices between the thickness of litter in Exp. 1–1 and the soil depth in Exp. 1–2. The theoretical basis of this analysis is described later in the **Materials and Methods**. In this experiment, 12 dowels made of *C. japonica* with a 4-cm diameter and 1-m length were stored in a pool of water for 1 month to obtain high water contents. We then removed the dowels from the pool, and sealed their cut ends with silicone to prevent water loss. We buried the dowels horizontally at depths of 10, 20, 30, and 50 cm, at 50-cm intervals, with three replicates at each depth (Fig. 3a). They were also scanned along transects perpendicular to the long axis of the dowels. The values of the GPR indices were the average of the values for the three replicates at each depth.

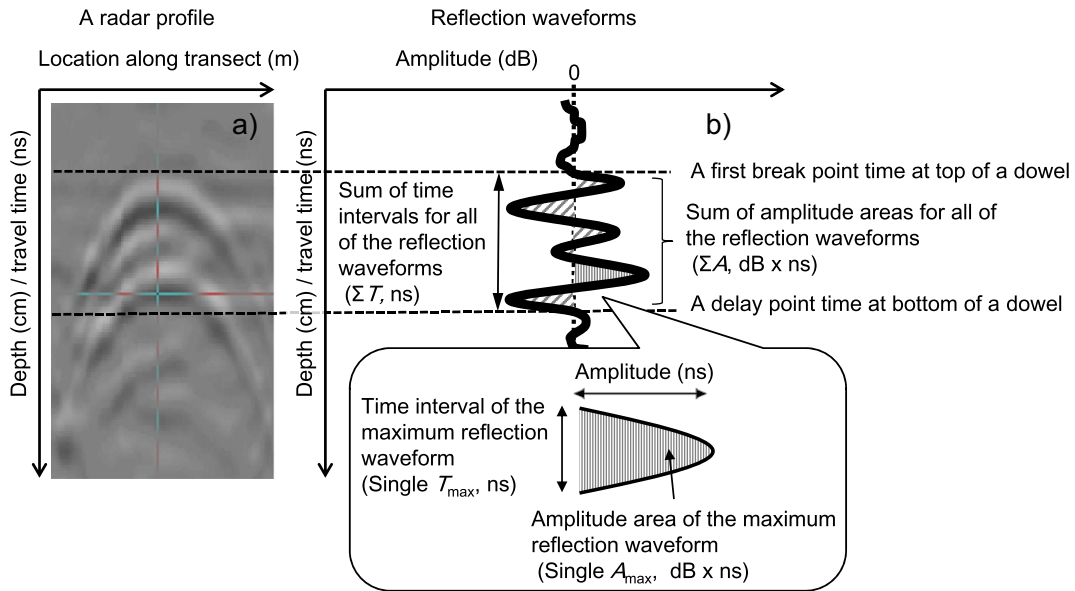


**Fig. 1** A representative 900 MHz radar profile and extraction of the radar wave parameters (modified from Tanikawa et al. 2013). **a** A representative reflected hyperbola in a radar profile of a target (a wooden dowel) buried at a depth of 30 cm; **b** the reflection waveforms and the four waveform parameters extracted in this study: the sum of the time intervals between zero crossings for all

of the reflection waveforms ( $\Sigma T$ , ns); the time interval between zero crossings of the maximum reflection waveform (Single  $T_{max}$ , ns); the sum of the amplitude areas for all of the reflection waveforms ( $\Sigma A$ , dB  $\times$  ns); and the amplitude area for the maximum reflection waveform (Single  $A_{max}$ , dB  $\times$  ns)

Experiment 2 was designed to determine whether the GPR signals obtained from different plant species could be used to distinguish the species. We investigated the

appearance of the reflections in the radar profiles and the values of the GPR indices using roots from conifers and hardwoods, as well as the rhizomes of bamboo. We

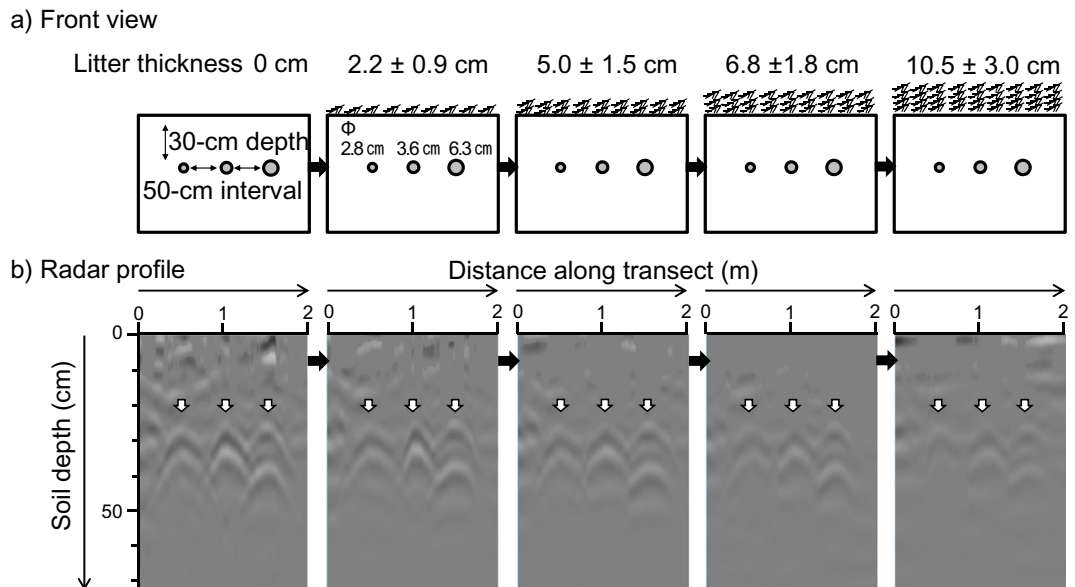
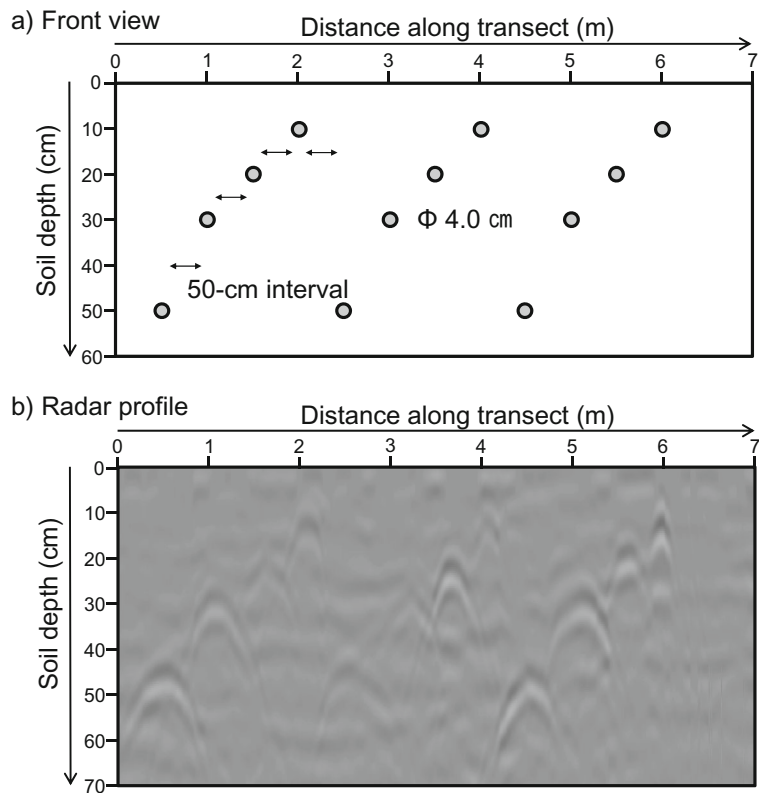


**Fig. 2** Illustration of the design of Experiment 1-1 and representative radar profiles that demonstrate the influence of leaf litter. **a** Position of the three roots (*C. japonica*) in the front view; **b** the corresponding radar profiles. The ground surface was covered by a

litter layer with mean depths ranging from 0 to 10.5 cm. White arrows indicate that the roots were visually detected in the radar profiles

**Fig. 3** Illustration of the design of Experiment 1–2, which was designed to investigate the effects of soil depth on the radar profiles. **a** Position of the 12 dowels (*C. japonica*) in front view; **b** a representative radar profile. Dowels were buried at four depths



examined two roots each of *Pinus densiflora* and *C. japonica* (coniferous) and of *Quercus serrata* (hardwood), in Experiment 2–1, and one root of *C. japonica* and two rhizomes of *Phyllostachys pubescens* (bamboo) in Experiment 2–2 (Fig. 4a, b, Supplementary Table S1). They were buried horizontally at 50-cm intervals at a depth of 30 cm, and scanned along three parallel transects, separated by 10 cm, perpendicular to the long axis of the roots. Measured GPR indices were reported as the average of the three scanning values. We performed simple linear regression analysis for the relationship between root diameter and the values of the GPR indices using version 6 of the Statistica software (StatSoft, Tulsa, Oklahoma, USA).

#### Data collection

For our measurements, we used a field-portable GPR system with a 900 MHz antenna (SIR 10H or SIR 3000; Geophysical Survey Systems, Inc., Nashua, NH, USA). The device has a bowtie dipole configuration. The antenna was calibrated for gain at five points: each was 9 dB in Experiment 1–1 and 1–2; at 0, 0, 10, 30, and

40 dB in Experiment 2. The gain was unified to compare the attenuation of the GPR index values in Experiment 1, but was adjusted to obtain clear hyperbolas for the GPR signals in Experiments 2. The soil dielectric constant was set to 9.0 (dimensionless), which was the value used under the same conditions in previous research at the same site (Hirano et al. 2009; Tanikawa et al. 2013). Radar profiles were collected as 8-bit data files, with a range of 15 ns along each transect. After GPR scanning, 100-cm<sup>3</sup> soil cores were collected under the transect to measure the volumetric soil water content in each experiment. Soil and root samples were oven-dried at 105 and 80 °C, respectively, for 3 to 4 days and then weighed to calculate the wood densities and volumetric water contents. The bulk density and the volumetric water content of the sandy soil fell within a small range: from 1.3 to 1.4 g cm<sup>-3</sup> and from 10.5 to 14.4 %, respectively (Supplementary Table S2). The volumetric water contents of the root samples for Experiments 1–1 were 53.7 % for Root 1, 52.8 % for Root 2, and 59.9 % for Root 3. Those of the dowels used in Experiment 1–2 ranged from 13.4 to 26.9 % (19.4 ± 4.3 %, *n* = 12, mean ± standard deviation). The wood density and

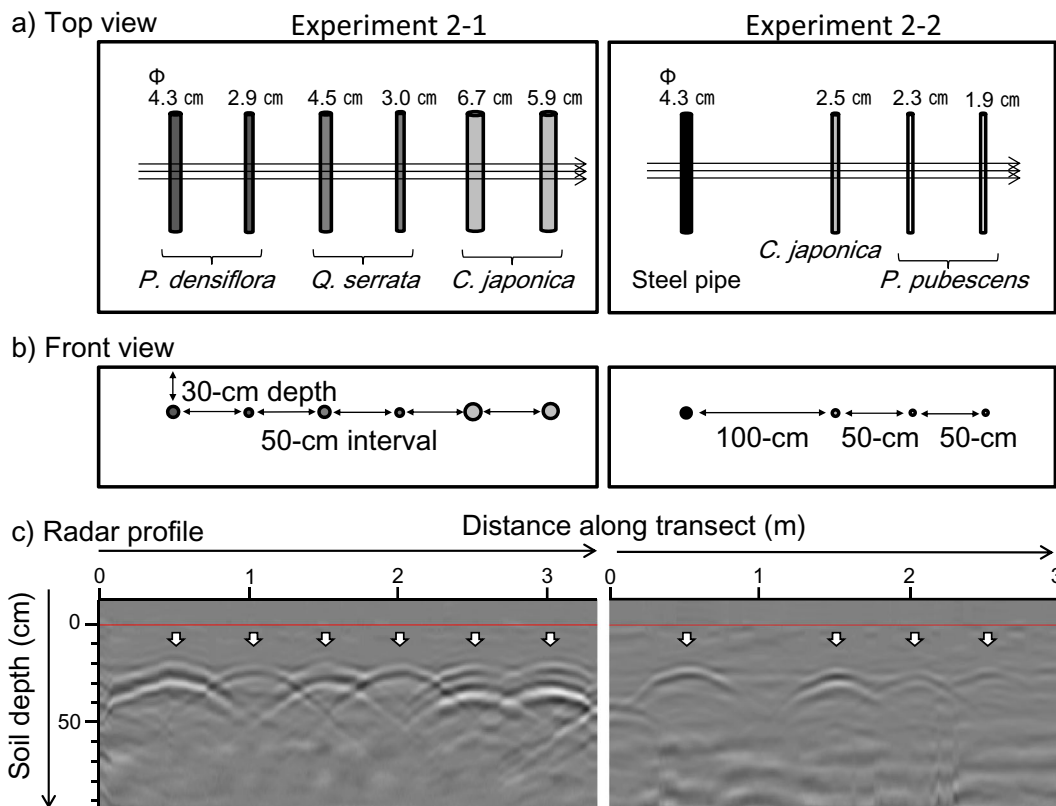


**Fig. 4** Illustration of the design of Experiment 2 to reveal the effect of plant species on the radar profile. **a** Positions of the roots and rhizomes of the four species, and of a steel pipe used as a

control; **b** front view; and **c** representative radar profiles. White arrows indicate that the roots or rhizomes were visually detected

volumetric water content of the roots and rhizomes in Experiment 2 ranged from 0.42 to 0.60 g cm<sup>-3</sup> and from 29.7 to 64.8 %, respectively (Supplementary Table S1).

#### Data processing

Radar profile normalization and filtration were performed using the RADAN software for Windows (Geophysical Survey Systems). Applying a background-removal filter eliminated the parallel bands that we observed in the scans as a result of reflections from planes such as the ground surface, soil horizons, and bands of low-frequency noise (Butnor et al. 2003). We attempted to identify the target materials (i.e., the roots, rhizomes, dowels, steel pipes) based on the presence of visible hyperbolas and reflection waveforms with higher amplitude than the surrounding area in the radar profiles.

We calculated two forms of each of the two main GPR indices defined by Tanikawa et al. (2013):  $\Sigma T$ , which is the sum of the time intervals between zero crossings ( $T$ ) for all of the reflection waveforms within

the range from the first break time at the top to the delay point time at the bottom, and  $\Sigma A$ , which is the sum of the individual values for the amplitude area ( $A$ ) (Fig. 1). We also recorded Single  $T_{\max}$ , the  $T$  value for the maximum reflection waveform, and Single  $A_{\max}$ , which was the  $A$  value for the maximum reflection waveform.

#### Theory for experiment 1

Because the  $A$  values decrease with increasing depth of the target (Cui et al. 2013), we hypothesized that the  $A$  values would decrease with increasing leaf litter accumulation due to the resultant increase in the distance between the antenna and the target (Supplementary Fig. S1). Cui et al. (2013) proposed the following eq. to represent the influence of root depth on the  $A$  values:

$$A(t) = C \exp(-\alpha * t) \quad (1)$$

where  $A(t)$  is the value of the amplitude of the two-way travel time ( $t$ );  $C$  is the true amplitude (without energy

attenuation) at a depth of 0 cm;  $\alpha^*$  is an attenuation factor, which can be estimated by performing an exponential regression fitting of the amplitude area as a function of the wave travel time. Litter thickness was a variable but root depth was constant at a depth of 30 cm in Experiment 1–1 (Supplementary Fig. S1). Thus, litter thickness ( $l$ ) was an independent variable determining the wave travel time ( $t$ ). To estimate  $\alpha^*$  of the litter layer ( $\alpha_{\text{litter}}^*$ ), we assigned  $A$  values into  $A(t)$  and litter thickness ( $l$ ) into  $t$  in Eq. (1), as follows:

$$A(l) = C_{\text{litter}} \exp(-\alpha_{\text{litter}}^* \times l) \quad (2)$$

where  $C_{\text{litter}}$  is the amplitude without energy attenuation at a litter thickness of 0 cm. We calculated the coefficients  $\alpha_{\text{litter}}^*$  and  $C_{\text{litter}}$  by regression of the measured  $A$  values in Eq. (2) using version 6.03 of the IGOR Pro software (WaveMetrics, Inc., Portland, OR, USA). To confirm the independence of the  $T$  values from the litter's influence, we also fitted the  $T(l)$  values into Eq. (2) as the objective variable. We calculated the coefficient of determination ( $R^2$ ) and level of significance ( $P$ ) using version 6 of the Statistica software (StatSoft, Tulsa, Oklahoma, USA).

By rearranging Eq. (2), we obtain:

$$\frac{A(l)}{C_{\text{litter}}} = \exp(-\alpha_{\text{litter}}^* \times l) \quad (3)$$

Equation (3) indicates that the rate of reduction of  $A$  by the litter layer, which represents the ratio of the  $A$  values of the roots to  $C_{\text{litter}}$ , is represented by an exponential function of  $\alpha_{\text{litter}}^*$  and  $l$ . We then calculated the measured rate of reduction of  $A$  by the litter layer using the measured  $A$  values, and compared them with the rates predicted using Eq. (3).

Experiment 1–2 was designed to calculate the rate of reduction when the medium was a sandy soil without a litter layer, so that we could compare the result (with only soil attenuation) with that obtained in Experiment 1–1 (with leaf litter + soil attenuation). The attenuation factor  $\alpha_{\text{soil}}^*$  was determined by assigning  $A$  values into  $A(t)$  and soil depth ( $d$ ) into  $t$  in Eq. (1), as follows:

$$A(d) = C_{\text{soil}} \exp(-\alpha_{\text{soil}}^* \times d) \quad (4)$$

where  $C_{\text{soil}}$  is the true amplitude without energy attenuation at a depth of 0 cm in the soil. The rate of

reduction  $A(d)/C_{\text{soil}}$  can be calculated by rearranging Eq. (4) as follows:

$$\frac{A(d)}{C_{\text{soil}}} = \exp(-\alpha_{\text{soil}}^* \times d) \quad (5)$$

In the same manner as in Experiment 1–1, we fitted the measured  $A$  values to Eq. (4) by regression analysis using the IGOR Pro software, and then calculated the reduction rates caused by the soil matrix using Eq. (5). Because previous studies indicated that  $T$  values were independent of the depth in the soil (Barton and Montagu 2004; Cui et al. 2013), we did not perform the fitting of  $T$  values into Eq. (4) in Experiment 1–2.

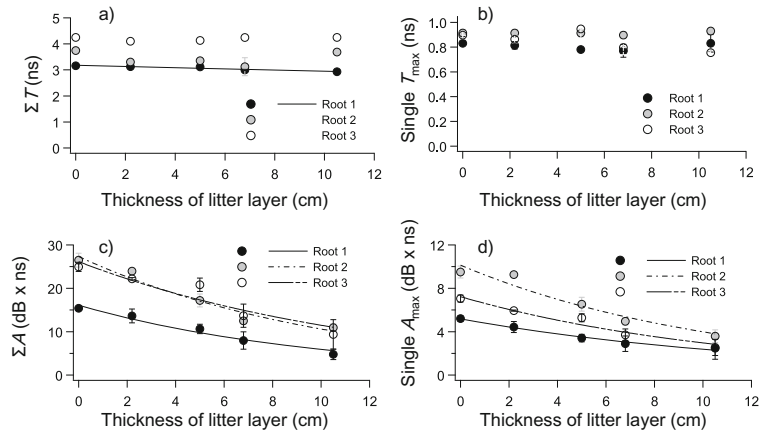
## Results

### Experiment 1: effects of the leaf litter layer

In Experiment 1–1, the distance between the GPR antenna and the buried roots was increased by the presence of a litter layer of variable thickness (Supplementary Fig. S1). The contrast between the hyperbolas in the radar profile (used to reveal the presence of a root) and the background weakened as the litter layer thickness increased (Fig. 2b). Nevertheless, the shapes of the hyperbolas were not distorted by the litter layer. Both  $\Sigma A$  and Single  $A_{\text{max}}$  decreased with increasing litter thickness, whereas  $\Sigma T$  and Single  $T_{\text{max}}$  were independent of this thickness (Fig. 5a–d). The  $T$  values ( $\Sigma T$  and Single  $T_{\text{max}}$ ) either did not confirm with Eq. (2) or the regression formulas were not significant, except for a significant regression of  $\Sigma T$  for root 1 (Table 1). All  $A$  values were significantly fitted to the corresponding equations (Table 1,  $P < 0.05$ ). The attenuation coefficient  $\alpha_{\text{litter}}^*$  in Eq. (2) ranged from 0.082 to 0.100 for  $\Sigma A$ , and from 0.078 to 0.093 for Single  $A_{\text{max}}$ . The only significant attenuation coefficient  $\alpha_{\text{litter}}^*$  for  $\Sigma T$  (for root 1) had a substantially lower value (0.007) than the  $A$  values, meaning that there was little attenuation by the litter.

In Experiment 1–2, the distance between the GPR antenna and the buried targets (dowels) increased with increasing depth in the soil matrix; with no litter layer, both  $\Sigma A$  and Single  $A_{\text{max}}$  decreased with increasing depth (Supplementary Fig. S2). The coefficient  $\alpha_{\text{soil}}^*$  in Eq. (4) averaged 0.046 for  $\Sigma A$  and 0.053 for Single  $A_{\text{max}}$  (Table 1).

**Fig. 5** Relationships between the GPR indices for the roots and litter layer thickness (mean ± standard deviation,  $n = 3$ ) in Experiment 1–1. **a** Sum of the time interval between zero crossings ( $\Sigma T$ ); **b** maximum  $T$  (Single  $T_{\max}$ ); **c** sum of the amplitude area ( $\Sigma A$ ); and **d** maximum  $A$  (Single  $A_{\max}$ ). Only statistically significant fitting lines are shown ( $P < 0.05$ ). Coefficients, RMSE, and  $R^2$  of the formulas are shown in Table 1



To compare the influence of litter thickness and soil depth on the  $A$  values, we compared the predicted and measured reduction rates of  $A$  using Eq. (3) for litter and Eq. (5) for the soil matrix. With a litter layer, both  $\Sigma A$

and Single  $A_{\max}$  had similar predicted reduction rates, ranging from 0.91 to 0.93 with a litter thickness of 1.0 cm, from 0.82 to 0.86 with a litter thickness of 2.0 cm, from 0.61 to 0.68 with a litter thickness of

**Table 1** Coefficients of Eq. (2)<sup>a</sup> and Eq. (4)<sup>b</sup> in Experiments 1–1 and 1–2 for the GPR indices

GPR index	Experiment	Medium	Target	Coefficient in Eq. (2) or Eq. (4) <sup>c</sup>		RMSE (ns for $T$ ; dB × ns for $A$ )	$R^2$
				Sample	$\alpha_{\text{litter}}^*$ or $\alpha_{\text{soil}}^*$		
$\Sigma T^d$	1–1	Litter	Root 1	0.007 ± 0.001	3.18 ± 0.03	0.03	0.90*
			Root 2	Not significant <sup>e</sup>		0.24	0.01
			Root 3	Did not conform <sup>f</sup>		–	–
Single $T_{\max}^d$	1–1	Litter	Root 1	Did not conform <sup>f</sup>		–	–
			Root 2	Not significant <sup>e</sup>		0.82	0.00
			Root 3	Not significant <sup>e</sup>		0.07	0.13
$\Sigma A$	1–1	Litter	Root 1	0.100 ± 0.012	16.1 ± 0.8	0.71	0.97**
			Root 2	0.095 ± 0.013	27.3 ± 1.4	1.26	0.96**
			Root 3	0.082 ± 0.019	26.1 ± 2.1	1.90	0.89*
	1–2	Soil	Dowel	0.046 ± 0.004	187 ± 12	3.12	0.99**
Single $A_{\max}$	1–1	Litter	Root 1	0.078 ± 0.006	5.2 ± 0.1	0.12	0.99***
			Root 2	0.093 ± 0.015	10.1 ± 0.6	0.58	0.94**
			Root 3	0.089 ± 0.013	7.2 ± 0.4	0.34	0.95**
	1–2	Soil	Dowel	0.053 ± 0.004	80.6 ± 5.6	1.29	0.99**

GPR ground penetrating radar RMSE root-mean-square error,  $R^2$  coefficient of determination

<sup>a</sup>  $A(l) = C_{\text{litter}} \exp(-\alpha_{\text{litter}}^* \times l)$

<sup>b</sup>  $A(d) = C_{\text{soil}} \exp(-\alpha_{\text{soil}}^* \times d)$

<sup>c</sup> mean ± SD,  $n = 3$  in Experiment 1–1;  $n = 12$  in Experiment 1–2

<sup>d</sup> Because previous studies indicated that the  $T$  values were independent of soil depth (Barton and Montagu 2004; Cui et al. 2013), we did not perform the fitting of  $T$  values into Eq. (4) in Experiment 1–2

<sup>e</sup> Although the data conformed with Eq. (2) using version 6.03 of the IGOR Pro software (WaveMetrics, Inc., Portland, OR, USA), the regression equation was not significant ( $P > 0.05$ )

<sup>f</sup> The IGOR Pro software judged that the data did not conform with Eq. (2)

\*, \*\* and \*\*\* indicate significance at  $P < 0.05$ ,  $P < 0.01$  and  $P < 0.001$ , respectively



5.0 cm, and from 0.37 to 0.46 with a litter thickness of 10.0 cm (Fig. 6). As with the results of the GPR scanning, the measured reduction rates of both  $\Sigma A$  and Single  $A_{\max}$  ranged from 0.84 to 0.98 with a litter thickness of 2.2 cm, from 0.65 to 0.83 with a litter thickness of 5.0 cm, and from 0.31 to 0.48 with a litter thickness of 10.5 cm. Thus, the errors in the reduction rates tended to be larger with shallower litter layers than with thicker layers. The reduction rates caused by the litter layer were higher than those caused by the soil matrix: the predicted reduction rates of  $A$  ranged from 0.90 to 0.91 at a depth of 2 cm in the soil matrix and from 0.59 to 0.63 at a depth of 10 cm.

### Experiment 2: effects of plant species

Roots of all four plant species were visually observed in the radar profiles (Fig. 4c). Although the intensity of the reflections from the rhizome of *P. pubescens* seemed to be weaker than reflections from roots of the other species, the shapes of the hyperbolas were similar (Fig. 4c). All GPR indices ( $\Sigma T$ , Single  $T_{\max}$ ,  $\Sigma A$ , and Single  $A_{\max}$ ) were significantly linearly correlated with the diameters of the roots or rhizomes based on data from all plant

species combined (Fig. 7).  $\Sigma A$  had the strongest correlation ( $R^2 = 0.98$ ), whereas Single  $T_{\max}$  had the weakest correlation ( $R^2 = 0.74$ ).

## Discussion

### Tree root detection by GPR

This study was conducted under ideal conditions (i.e., with control of the soil characteristics and litter layer), and therefore provided valuable knowledge of the effects of leaf litter and plant species on root detection using GPR. Our results clearly show that the leaf litter decreased the strength of radar images of the roots, and that the magnitude of this effect increased with increasing litter depth. Moreover, the characteristics of the reflected radar signal did not differ among the plant species.

In the leaf litter experiments, a thicker litter layer decreased the intensity of the root reflection compared with the background, but without distorting the shape of the hyperbolas in the radar profile (Fig. 2b). When the litter layer was thicker than 10 cm, the hyperbolas became difficult to recognize. Because the  $\Sigma T$  and Single  $T_{\max}$  values did not (with one exception) conform with Eq. (2) or produced a nonsignificant regression result, these parameters appear to be independent of the litter thickness (Fig. 5a, b, Table 1). Therefore, the influence of the litter can be ignored when the root reflections are visible (i.e., when the litter layer was less than 10 cm thick in the present study), and  $\Sigma T$  can be adopted to estimate root diameter (Fig. 7a). In contrast, it is necessary to be careful when using  $A$  values, since they decrease dramatically with increasing leaf litter thickness (Fig. 5c, d). When the leaf litter layer was less than 2 cm thick in this study, the underestimation of the  $A$  values caused by the litter layer ranged from 10 to 20 %. Thus, it is better to remove the litter layer before scanning, or to equalize its thickness within a sampling area to minimize the litter's influence on the root diameter estimated using  $A$  values. Even when removal of the litter layer is difficult, researchers should at least try to mitigate the effect of different litter thicknesses within a survey area; Fig. 7 shows a strong ability to predict root diameter when the litter layer is removed.

The reduction rate of  $A$  values caused by the litter layer was approximately 1.5 times higher than that caused by the depth of the sandy soil matrix at 10-cm

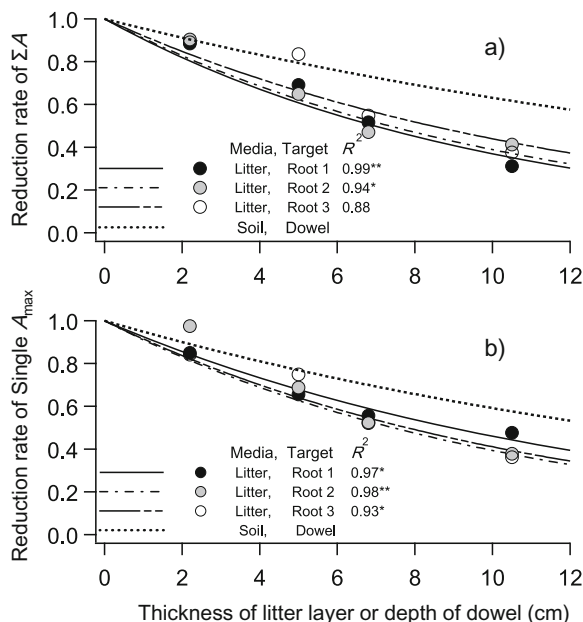
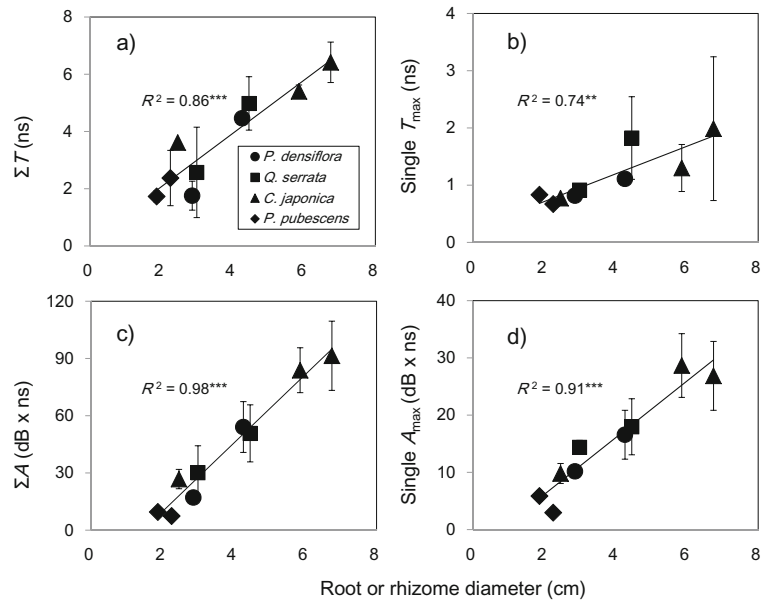


**Fig. 6** The reduction rates of the  $A$  values as a function of the thickness of the litter layer or the dowel depth in the soil matrix. **a**  $\Sigma A$  and **b** Single  $A_{\max}$ . Dots indicate the measured values and dotted lines indicate the predicted values for the dowels in Experiments 1–1 and 1–2.  $R^2$  is the coefficient of determination. \* and \*\* indicate significance at  $P < 0.05$  and  $P < 0.01$ , respectively

**Fig. 7** Relationships between the four GPR indices and the root or rhizome diameters for the four plant species (mean  $\pm$  standard deviation,  $n = 3$ ). **a** Sum of the time interval between zero crossings ( $\Sigma T$ ); **b** maximum  $T$  (Single  $T_{\max}$ ); **c** sum of the amplitude area ( $\Sigma A$ ); and **d** maximum  $A$  (Single  $A_{\max}$ ). A single linear regression line is shown based on data from all species combined. Significance: \*\* and \*\*\* indicate significance at  $P < 0.01$  and  $P < 0.001$ , respectively



thickness. The difference in this rate might have been increased due to the texture of the litter and the sandy soil; that is, the soil matrix was homogeneous and massive, whereas the litter layer of *C. japonica* leaves had many air spaces with a range of sizes in a multilayer structure, and the angles of the leaf surfaces also varied. This structural differences between the litter layer and the soil matrix might have resulted in the large variation in the reflected electromagnetic waves.

Although thicker litter layers and increasing soil depth might reduce the  $A$  values at different rates, the measured rate of reduction for the 2.2-cm-thick litter layer was similar to that of the soil matrix (Fig. 6a, b). The magnitude of the litter's influence on the  $A$  values appeared to be smaller when the layer was thinner. One possible explanation is that the disturbance in travel and reception of the electromagnetic waves caused by the litter layer might not be high when the layer is thin. Butnor et al. (2005) found that leaf litter blurred the visual characteristics of GPR images of roots, but did not quantify the effect. Our study is therefore the first we are aware of that quantified these effects using GPR indices.

Litter layers are composed of three predominant components: air, dry and wet cell walls, and water. The dielectric permittivity of these components equaled 1, 4.5, 22, and 81, respectively (al Hagrey 2012). The proportions of these components and their spatial distribution are likely to vary among both the

plant species and the seasons; thus different litter compositions will have different effects on GPR images. The homogeneous litter used in the present experiments would have limited the effects of variation in litter characteristics. In forest ecosystems, groundcover plants (e.g., mosses, clover, and grasses) on the forest floor also retain air and moisture. Since these properties of the understory are similar to those of the litter, groundcover plants may affect the detection accuracy of the target tree roots in a GPR survey. Further studies using a range of soil types, tree species with different litter structures, and various vegetation types will be needed to clarify the influence of litter on GPR detection under field conditions.

Although radar reflections vary in response to changes in the water content, air content, and content of other buried materials (Gormally et al. 2011), all the plant species that were used in Experiment 2 produced clear but similar hyperbolas in the radar profiles (Fig. 4c). One possible reason might be that the spatial scale of the anatomical variation is smaller than the resolution of the GPR detection. Both the  $T$  values (traveling time) and the  $A$  values (signal strength) were determined primarily by the root or rhizome diameters for all four species despite differences in their root or rhizome anatomy (Fig. 7). This probably resulted from similarities in the volumetric water contents and wood densities of the sample roots and rhizomes (Supplementary Table S1). When the distribution and biomass of tree roots are

estimated using GPR, the relationships between the GPR indices and the root or rhizome diameter (which would be proportional to their biomass) need to be established by means of partly destructive sampling (Hirano et al. 2012; Wu et al. 2014). Before the present study, the GPR indices, which were based on extraction of the number of pixels after a Hilbert transformation, were correlated with root biomass (e.g., Butnor et al. 2003) and with root diameter (e.g., Dannoura et al. 2008) in one species at a forest site. Borden et al. (2014) recently showed that the number of pixels after a Hilbert transformation was related to the root biomass for four different tree species. Our results suggest that root diameter could be estimated from GPR indices across plant species. In other words, it may not be necessary to establish species-specific relationships, which will allow researchers to minimize the destructive sampling of roots.

#### Implications for using $T$ and $A$ values to estimate root diameter

In the GPR method, the major advantage of adopting  $\Sigma T$  for predicting root sizes and distributions is that this index depends only on the geometric dimensions of the reflector and is independent of the signal strength (Cui et al. 2011). Thus,  $\Sigma T$  is independent of root orientation (Tanikawa et al. 2013), the root and soil water content (Hirano et al. 2009; Cui et al. 2011; Guo et al. 2013), root depth (Barton and Montagu 2004; Cui et al. 2013), and the thickness of the leaf litter layer (the present study). Although Single  $T_{\max}$  was significantly correlated with root diameter in the present study (Fig. 7b), this was inconsistent with our previous result (Tanikawa et al. 2013). Therefore,  $\Sigma T$  may be a more robust index of root diameter (and thus, of biomass). Nevertheless, the  $\Sigma T$  error could increase if the points at the first signal break (root top) and the delay (root bottom) are incorrectly extracted. In contrast to  $T$  values,  $A$  values ( $\Sigma A$ , Single  $A_{\max}$ ) have been adopted to estimate root diameter and biomass (Barton and Montagu 2004; Hirano et al. 2009; Cui et al. 2011, 2013; Guo et al. 2013; Tanikawa et al. 2013), even though the results suggest that these indices depend strongly on the conditions of the target materials and their surroundings. Despite this disadvantage,  $A$  values might be easier to extract from the radar profiles and more suitable than the  $T$  values for

developing and analyzing large GPR datasets in forests. Therefore, it is necessary to elucidate the effects of in-situ forest factors on  $A$  values under controlled conditions.

## Conclusions

Our results provide important new information on the influence of the litter layer and plant species on the detection and quantification of roots using GPR surveys. The presence of leaf litter clearly decreased root detection and quantification. The GPR data we examined could not distinguish among the roots of different plant species. Of the GPR indices we investigated, the  $A$  value decreased dramatically as the litter layer thickness increased, leading to an increasingly large underestimation of root diameter. In contrast, the  $T$  value was robust against the influence of litter. In addition, the root orientation, differences in water content between the roots and the soil, and root depth are likely to affect the  $A$  values. Hence, if  $A$  values are adopted to estimate root diameter or biomass, there is a risk of underestimation in GPR surveys of forest ecosystems. The effects of each of the abovementioned factors on  $A$  values in root detection can be corrected using recently reported methods (Cui et al. 2013; Tanikawa et al. 2013, 2014; Guo et al. 2013, 2015), but an integrative approach that corrects for the effects of all of these factors simultaneously has not yet been considered, and remains a challenge for future research. Therefore, further comprehensive studies will be needed to establish a method that accounts for these effects and improves the suitability of GPR for surveys in forests.

**Acknowledgments** We thank Y. Kanazawa (Kobe University), M. Ishii and T. Igarashi (KANSO Technos), M. Hiraoka (Tokyo University of Agriculture and Technology), and S. Asano, U. Kurokawa, T. Chikaguchi, S. Narayama, M. Tanaka, Y. Shimada, N. Makita, H. Hagino, and the other members of FFPRI for their help with data analysis and the field experiments. We also thank M. Ohashi (University of Hyogo) and Y. Matsuda (Mie University) for providing comments on an early draft of this manuscript. We additionally thank three reviewers for their critical comments on an earlier draft of the manuscript. We are grateful for financial support from Grants-in-Aid for Scientific Research from the Ministry of Education, Culture, Sports, Science and Technology (MEXT), Japan (No. 22380090, 25252027). This study was also supported by the Program for Supporting Activities for Female Researchers, which is funded by MEXT's Special Coordination Fund for Promoting Science and Technology.

## References

- al Hagrey SA (2012) Geophysical imaging techniques. In: Mancuso S (ed) Measuring roots, an updated approach. Springer-Verlag, Berlin Heidelberg, pp. 151–188
- Barton CM, Montagu KD (2004) Detection of tree roots and determination of root diameters by ground penetrating radar under optimal conditions. *Tree Physiol* 24:1323–1331. doi:10.1093/treephys/24.12.1323
- Borden KA, Isaac ME, Thevathasan NV, Gordon AM, Thomas SC (2014) Estimating coarse root biomass with ground penetrating radar in a tree-based intercropping system. *Agrofor Syst* 88:657–669. doi:10.1007/s10457-014-9722-5
- Brunner I, Godbold DL (2007) Tree roots in a changing world. *J For Res* 12:78–82. doi:10.1007/s10310-006-0261-4
- Butnor JR, Doolittle JA, Kress L, Cohen S, Johnsen KH (2001) Use of ground-penetrating radar to study tree roots in the southeastern United States. *Tree Physiol* 21:1269–1278. doi:10.1093/treephys/21.17.1269
- Butnor JR, Doolittle JA, Johnsen KH, Samuelson L, Stokes T, Kress L (2003) Utility of ground-penetrating radar as a root biomass survey tool in forest systems. *Soil Sci Soc Am J* 67:1607–1615. doi:10.2136/sssaj2003.1607
- Butnor J, Roth B, Johnsen K (2005) Feasibility of Using Ground-penetrating Radar to Quantify Root Mass in Florida's Intensively Managed Pine Plantations. FBRC Report #38
- Butnor JR, Barton C, Day FP, Johnsen KH, Mucciardi AN, Schroeder R, Stover DB (2012) Using ground-penetrating radar to detect tree roots and estimate biomass. In: Mancuso S (ed) Measuring roots, an updated approach. Springer-Verlag, Berlin Heidelberg, pp. 213–245
- Cermak J, Hruska J, Martinkova M, Prax A (2000) Urban tree root systems and their survival near houses analyzed using ground penetrating radar and sap flow techniques. *Plant Soil* 219:103–116. doi:10.1023/A:1004736310417
- Cheng NF, Tang HWC, Ding XL (2014) A 3D model on tree root system using ground penetrating radar. *Sustain Environ Res* 24:291–301
- Cox KD, Scherm H, Serman N (2005) Ground-penetrating radar to detect and quantify residual root fragments following peach orchard clearing. *Hort Technol* 15:600–607
- Cui XH, Shen JS, Cao X, Chen XH, Zhu XL (2011) Modeling tree root diameter and biomass by ground-penetrating radar. *Sci China Earth Sci* 54:711–719. doi:10.1007/s11430-010-413-z
- Cui X, Guo L, Chen J, Chen X, Zhu X (2013) Estimating tree-root biomass in different depths using ground-penetrating radar: evidence from a controlled experiment. *IEEE Trans Geosci Remote Sens* 51:3410–3423. doi:10.1109/TGRS.2012.2224351
- Dannoura M, Hirano Y, Igarashi T, Ishii M, Aono K, Yamase K, Kanazawa Y (2008) Detection of *Cryptomeria japonica* roots with ground penetrating radar. *Plant Biosyst* 142:375–380. doi:10.1080/11263500802150951
- Dixon RK, Brown S, Houghton RA, Solomon AM, Trexler MC, Wisniewski J (1994) Carbon pools and flux of global forest ecosystems. *Science* 263:185–189. doi:10.1126/science.263.5144.185
- Fan CC, Lai YF (2014) Influence of the spatial layout of vegetation on the stability of slopes. *Plant Soil* 377:83–95. doi:10.1007/s11104-012-1569-9
- Ghestem M, Veylon G, Bernard A, Vanel Q, Stokes A (2014) Influence of plant root system morphology and architectural traits on soil shear resistance. *Plant Soil* 377:43–61. doi:10.1007/s11104-012-1572-1
- Giadrossich F, Schwarz M, Cohen D, Preti F, Or D (2013) Mechanical interactions between neighbouring roots during pullout tests. *Plant Soil* 367:391–406. doi:10.1007/s11104-012-1475-1
- Gormally KH, McIntosh MS, Mucciardi AN (2011) Ground-penetrating radar detection and three-dimensional mapping of lateral macropores: I. Calibration. *Soil Sci Soc Am J* 75:1226–1235. doi:10.2136/sssaj2010.0339
- Groisman PY, Karl TR, Easterling DR, Knight RW, Jamason PF, Hennessy KJ, Suppiah R, Page CM, Wibig J, Fortuniak K, Razuvaev VN, Douglas A, Forland E, Zhai PM (1999) Changes in the probability of heavy precipitation: important indicators of climatic change. *Clim Chang* 42:243–283. doi:10.1023/A:1005432803188
- Guo L, Lin H, Fan B, Cui X, Chen J (2013) Impact of root water content on root biomass estimation using ground penetrating radar: evidence from forward simulations and field controlled experiments. *Plant Soil* 371:503–520. doi:10.1007/s11104-013-1710-4
- Guo L, Wu Y, Chen J, Hirano Y, Tanikawa T, Li W, Cui X (2015) Calibrating the impact of root orientation on root quantification using ground-penetrating radar. *Plant Soil* 395:289–305. doi:10.1007/s11104-015-2563-9
- Hirano Y, Dannoura M, Aono K, Igarashi T, Ishii M, Yamase K, Makita N, Kanazawa Y (2009) Limiting factor in the detection of tree roots using ground-penetrating radar. *Plant Soil* 319:15–24. doi:10.1007/s11104-008-9845-4
- Hirano Y, Yamamoto R, Dannoura M, Aono K, Igarashi T, Ishii M, Yamase K, Makita N, Kanazawa Y (2012) Detection frequency of *Pinus thunbergii* roots by ground-penetrating radar is related to root biomass. *Plant Soil* 360:363–373. doi:10.1007/s11104-012-1252-1
- IPCC (2012) Summary for Policymakers. In: CB F, Barros V, TF S, Qin D, DJ D, KL E, MD M, KJ M, G-K P, SK A, Tignor M, PM M (eds) Managing the risks of extreme events and disasters to advance climate change adaptation. A special report of working groups I and II of the intergovernmental panel on climate change. Cambridge University Press, Cambridge, pp. 1–19
- Jackson RB, Canadell J, Ehleringer JR, Mooney HA, Sala OE, Schulze ED (1996) A global analysis of root distributions for terrestrial biomass. *Oecologia* 108:389–411. doi:10.1007/BF00333714
- Karizumi N (2010) The latest illustrations of tree roots. Seibundoshinkosha, Tokyo, 937 pp
- Khalilnejad A, Ali FH, Osman N (2012) Contribution of the root to slope stability. *Geotech Geol Eng* 30:277–288. doi:10.1007/s10706-011-9446-5
- Paul KI, Jacobsen K, Koul V, Leppert P, Smith J (2008) Predicting growth and sequestration of carbon by plantations growing in regions of low-rainfall in southern Australia. *For Ecol Manag* 254:205–216. doi:10.1016/j.foreco.2007.08.003
- Preston NJ, Crozier MJ (1999) Resistance to shallow landslide failure through root-derived cohesion in east coast hill country soils, North Island, New Zealand. *Earth Surf Process Landf* 24:665–675. doi:10.1002/(SICI)1096-9837(199908)24:8<665::AID-ESP980>3.0.CO;2-B

- Schenk HJ, Jackson RB (2002) Rooting depths, lateral root spreads and below-ground/above-ground allometries of plants in water-limited ecosystems. *J Ecol* 90:480–494. doi:[10.1046/j.1365-2745.2002.00682.x](https://doi.org/10.1046/j.1365-2745.2002.00682.x)
- Stover DB, Day FP, Butnor JR, Drake BG (2007) Effect of elevated CO<sub>2</sub> on coarse root biomass in Florida Scrub detected by ground-penetrating radar. *Ecology* 88:1328–1334. doi:[10.1890/06-0989](https://doi.org/10.1890/06-0989)
- Tanikawa T, Hirano Y, Dannoura M, Yamase K, Aono K, Ishii M, Igarashi T, Ikeno H, Kanazawa Y (2013) Root orientation can affect detection accuracy of ground-penetrating radar. *Plant Soil* 373:317–327. doi:[10.1007/s11104-013-1798-6](https://doi.org/10.1007/s11104-013-1798-6)
- Tanikawa T, Dannoura M, Yamase K, Ikeno H, Hirano Y (2014) Reply to: “Comment on root orientation can affect detection accuracy of ground-penetrating radar”. *Plant Soil* 380:445–450. doi:[10.1007/s11104-014-2136-3](https://doi.org/10.1007/s11104-014-2136-3)
- Trenberth KE (1999) Conceptual framework for changes of extremes of the hydrological cycle with climate change. *Clim Chang* 42:327–339. doi:[10.1023/A:1005488920935](https://doi.org/10.1023/A:1005488920935)
- Wu Y, Guo L, Cui X, Chen J, Cao X, Lin H (2014) Ground-penetrating radar-based automatic reconstruction of three-dimensional coarse root system architecture. *Plant Soil* 383:155–172. doi:[10.1007/s11104-014-2139-0](https://doi.org/10.1007/s11104-014-2139-0)